Experiments in Fluids 15, 209–218 (1993)

Experiments in Fluids

A calibration technique for multiple-sensor hot-wire probes and its application to vorticity measurements in the wake of a circular cylinder

B. Marasli, P. Nguyen*, J. M. Wallace

Department of Mechanical Engineering, University of Maryland, College Park, MD 20742, USA

Received: 26 October 1992 / Accepted: 4 April 1993

Abstract. A calibration technique for multiple-sensor hot-wire probes is presented. The technique, which requires minimal information about the probe geometry, is tested using a four-sensor and a twelve-sensor probe. Two data reduction algorithms are introduced. The first one assumes a uniform velocity over the probe sensing-volume and is applied to the four-sensor probe measurements. The second one assumes a uniform velocity gradient over the sensing volume of the probe. The procedure, when applied to the twelve-sensor probe, is shown to measure the velocity gradient components successfully. In both algorithms, the unknowns (velocity and velocity gradient components) are obtained by solving the resulting systems of nonlinear algebraic equations in a least-squares sense. The performances of the probes and the algorithms are tested with measurements in the wake of a circular cylinder. The statistics and spectra show that the twelve-sensor probe is successful in the simultaneous measurement of all three components of the velocity and all three components of the vorticity vectors.

1 Introduction

Since the hot-wire response equations are nonlinear, the solutions are not necessarily unique in general. A triple-sensor probe is known to yield nonunique solutions at high angles-of-attacks. Lekakis et al. (1989) presented a signal interpretation technique and uniqueness domains for triple-sensor probes with certain geometries. Samet and Einav (1987) used a fourth sensor in order to solve the uniqueness problem. Döbbeling et al. (1990) showed that a four-sensor would give a larger acceptability cone (approaching 90° half angle) than a triple-sensor probe and that it would yield a unique solution inside this angular range.

Vorticity, which is defined as the curl of the velocity field, is known to be an important quantity related to the structure of the turbulent flow field. However, since vorticity involves the gradients of the velocity field, until recently its measurements has been limited to a very few simple cases. Vukoslavčević et al. (1991) describe a miniature probe with nine hot-wire sensors which is capable of measuring the velocity and vorticity vectors with a spatial resolution of about six Kolmogorov microscales in the buffer layer of a turbulent boundary layer. Their probe is composed of three arrays of triple-sensor probes and performed well provided that the angle between the velocity vector and the probe axis is less than approximately 20°. When the angle-of-attack is about 20° the uniqueness problems inherent with the nonlinear response equations make the reliability of the results questionable. In order to overcome the uniqueness problems of the nine-sensor probe, a twelve-sensor probe was constructed by P. Vukoslavčević. The probe consists of three four-sensor arrays and, as will be shown in this article, it eliminates the problems encountered by the nine-sensor probe.

The quality of any hot-wire measurement technique starts with the quality of the calibration. Regardless of the technique used, the calibration of hot-wire probes deteriorates with time due to various reasons such as temperature variations, drift in electronics, impurities in the flow, etc. Therefore, a technique which permits the calibration to be completed within a short period of time, is essential. A multi-sensor probe often has wires oriented at various roll angles. Accurate determination of the individual sensor orientations in the probe can be quite difficult. One of the objectives of the current project was to develop a calibration and data reduction scheme which required minimal information about probe geometry and enabled relatively short calibration times.

In this article we present a calibration technique for multiple-sensor hot-wire probes. The technique is tested using a four-sensor probe and the twelve-sensor probe, both constructed by P. Vukoslavčević. Two data reduction algorithms, which take advantage of today's abundant desktop computing powers, are presented. The performances of the probes and the algorithms are tested with measurements in the wake of a circular cylinder.

* Permanent address: Propulsor Technology Branch, David Taylor Model Basin, Bethesda, MD 20084

Correspondence to: B. Marasli

2 Experimental apparatus

2.1 The four- and twelve-sensor probes

The four-sensor probe (Fig. 1), consists of two x-arrays, one each located with the horizontal and vertical orientations. The 2.5 μm diameter tungsten sensors are welded on eight nickel plated 100 μm diameter tungsten prongs which have been tapered to 40 μm at the tips. The prongs are reinforced by epoxy glue 15 mm from the probe tip for improved strength.

The twelve-sensor probe (Fig. 2) is an extension of the nine-sensor probe described by Vukoslavčević et al. (1991). The probe consists of three four-sensor arrays each placed at the vertices of an equilateral triangle.

2.2 Experimental facility and instrumentation

The measurements were carried out in the University of Maryland Turbulence Research Laboratory open-return wind tunnel. The octagonal test-section of the tunnel is 120 cm wide and 70 cm high with corner fillets to avoid secondary flows. The tunnel can deliver stable flow-speeds in the range of 1–5.5 m/s with a free-stream turbulence level of 0.5%. The circular cylinder was mounted horizontally along the 120 cm span of the tunnel where the velocity was uniform within 1.5%. The probes were mounted on an extension arm which placed the sensors upstream of any regions of flow interference caused by the traversing mechanism. For calibration, the probes were placed in the potential core of an air-jet which accommodated a specially designed pitch and yaw mechanism attached to its nozzle. The mechanism enabled the probe to be subjected to uniform flows at pitch and yaw angles (Fig. 3) in the range $\pm 20°$. The probes were calibrated before and after the measurements and were checked for possible drift. The effects of moving the probes from the calibration jet to the wind tunnel were carefully studied and found to be insignificant. The probes were connected to AA Lab Systems constant-temperature anemometers with built in gain, offset and low-pass filter circuitry. A Data Translation 12 channel, 12 bit A/D converter with simultaneous sample and hold capability connected to a PDP 11/23 microcomputer was used to acquire data. The processing was done on a Sun Sparcstation.

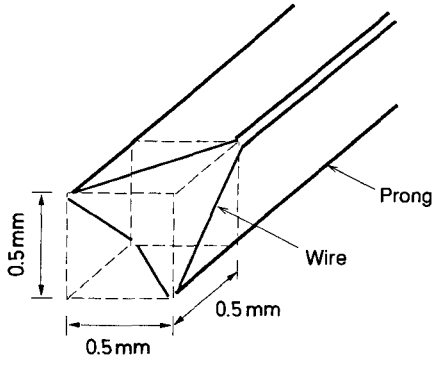

Fig. 1. Sketch of the four-sensor probe

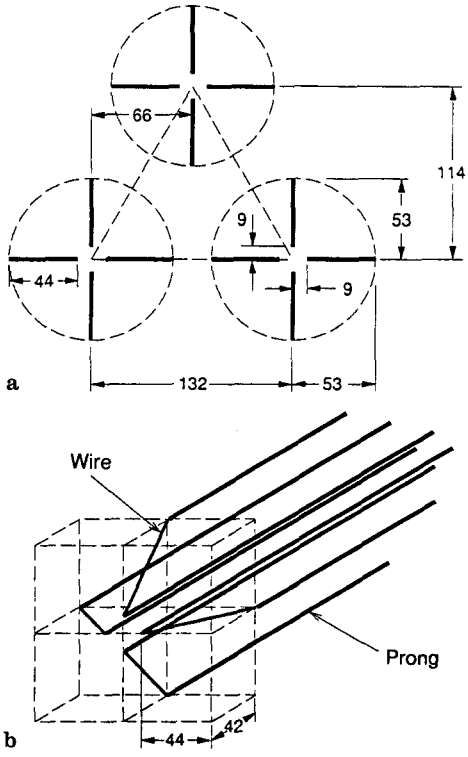

Fig. 2a and b. Sketch of the twelve-sensor vorticity probe. **a** Front view; **b** perspective view of one four-sensor array. All dimensions are in 1/100 mm

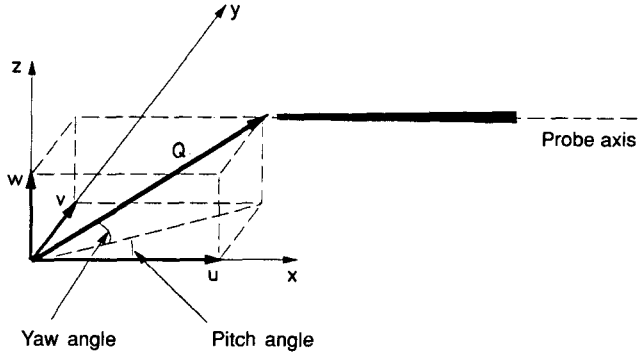

Fig. 3. A sketch defining the pitch and yaw angles

3 The calibration procedure

We start with the Jorgensen (1971) directional response equation

$$U_{eff}^2 = u_N^2 + k^2 u_T^2 + h^2 u_B^2, \quad (1)$$

where u_N, u_T and u_B are the normal, tangential and binormal components of the velocity with respect to the sensor (Fig. 4) and k and h are the tangential and binormal cooling coefficients respectively. In accordance with Vagt (1979), Adrian et al. (1984) and Lekakis et al. (1989), since only relatively small pitch (α) and yaw (β) angles ($-20° \leq \alpha, \beta \leq 20°$) are considered, k and h are assumed to be constants. It is desirable to express U_{eff} in terms of the velocity components u, v and w with respect to a rectangular coordinate system fixed to the laboratory. For an inclined sensor, u_N, u_T and u_B can be written as

$$u_N = N_1 u + N_2 v + N_3 w, \tag{2}$$

$$u_T = T_1 u + T_2 v + T_3 w, \tag{3}$$

$$u_B = B_1 u + B_2 v + B_3 w, \tag{4}$$

where N_i, T_i and B_i ($i = 1, 2, 3$) are coefficients of the coordinate transformation from the laboratory coordinates to the coordinates along the sensor which, in principle, can be determined by careful measurement of the sensor orientation with respect to the probe axis. For a multi-sensor miniature probe, accurate determination of the orientation of the individual sensors is possible but difficult. It is better to treat the constants N_i, T_i and B_i as unknowns and determine them through the calibration process

Substitution of Eqs. (2)–(4) into Eq. (1) yields:

$$U_{eff}^2 = b_0 u^2 + b_1 v^2 + b_2 w^2 + b_3 uv + b_4 uw + b_5 vw, \tag{5}$$

where b_m ($m = 0$–5) are functions of N_i, T_i, B_i, k and h. Hence, the geometrical and thermal coefficients are lumped together to be determined by direct calibration.

The effective cooling velocity, U_{eff}, has traditionally been related to the anemometer bridge voltage via King's (1914) law. In the present scheme a fourth order polynomial is used instead, in which case the sensor response equation becomes

$$u^2 - K_1 v^2 - K_2 w^2 - K_3 uv - K_4 uw - K_5 vw = P(e), \tag{6}$$

where

$$P(e) \equiv A_0 + A_1 e + A_2 e^2 + A_3 e^3 + A_4 e^4. \tag{7}$$

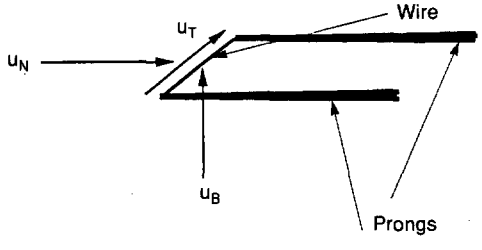

Fig. 4. A sketch defining the normal (u_N), tangential (u_T) and binormal (u_B) components of the velocity

Here e corresponds to the bridge voltage. We have divided throughout by b_0 to make the coefficient of u^2 unity.

The coefficients K_m ($m = 1$–5) and A_n ($n = 0$–4) can be obtained via calibration by subjecting the sensor to a uniform flow of variable but known magnitude Q at various known pitch (α) and yaw (β) angles (Fig. 3). The velocity components, $u \equiv (u, v, w)$, are then given by

$$u = Q \cos\alpha \cos\beta, \tag{8}$$

$$v = Q \sin\alpha \cos\beta, \tag{9}$$

$$w = Q \sin\beta. \tag{10}$$

A minimum of ten calibration points are required to solve for the unknowns K_m and A_n. In general, more calibration points will result in a better probe calibration. Variation of α and β for at least two speeds (Q) is recommended. Given a set of calibration velocities and the corresponding values of the anemometer bridge voltage e, the unknown coefficients can be determined by the method of least-squares. The linear system of equations resulting from the least-squares analysis is given in the Appendix.

A typical set of calibration data for one sensor is presented in Fig. 5. In this calibration set, the pitch and yaw angles were varied between $\pm 20°$ at two different speeds ($Q = 5.0$ and 3.2 m/s). In addition, the response of the wire was recorded at zero pitch and yaw for several speeds in the range 2.6–5.7 m/s for a total of 126 points. In Fig. 5, the ordinate values of the symbols correspond to the left-hand side of Eq. (6), where the velocity components are the known induced values given by Eqs. (8)–(10). The ordinate values of the solid line is the fourth order polynomial fit which represents the right-hand side of Eq. (6). Note that the data include points with combined pitch, yaw and speed variations. The fact that all points collapse on one curve is an indication that Jorgensen's equation is quite satisfactory in representing the response of a hot-wire in a combined pitch and yaw orientation as was also pointed out by Lekakis et al. (1989).

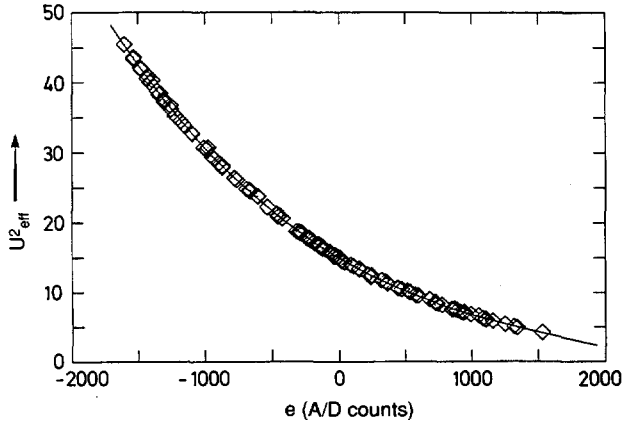

Fig. 5. Typical calibration data for one sensor of the twelve-sensor probe. ◇, measurements; ——, polynomial fit

4 Data reduction

4.1 Uniform velocity in the sensing volume – the four-sensor probe

In order to determine the instantaneous velocity vector in a turbulent flow at least three sensors are required to solve for the three unknowns u, v and w, assuming that the spatial resolution of the probe is sufficiently small so that the gradients across the sensing volume can be neglected. In order to avoid the uniqueness problem associated with the triple-sensor response equations (Döbbeling et al. 1990), the present data reduction scheme uses the information from all four sensors simultaneously and solves the overdetermined nonlinear system of equations in a least-square sense where a suitably defined error is minimized. We formulate the problem by rewriting Eq. (6) for each sensor in the probe as

$$f_j \equiv u^2 - K_{1j}v^2 - K_{2j}w^2 - K_{3j}uv - K_{4j}uw - K_{5j}vw - P_j(e_j) = 0, \tag{11}$$

where the subscript j denotes a sensor. For the four-sensor probe $j = 1$–4. In Eq. (11) K_{mj} and $P_j(e_j)$ are known from the calibration and the anemometer output voltage, and $u \equiv (u, v, w)$ is the unknown vector. Thus, we have a system of four nonlinear algebraic equations with three unknowns. For the rare cases where a solution satisfies all four equations represented by Eq. (11) exactly, f_j will be identically zero. The goal of the solution scheme is to determine u such that the error defined as

$$F = \sum_{j=1}^{4} f_j^2 \tag{12}$$

is minimized. A variety of techniques is available for the solution of nonlinear algebraic systems. The simplest one, which also turns out to be the most suitable one for the present application, is Newton's method, where after an initial guess for the unknown vector, the incremental correction, $\Delta \boldsymbol{u}$, to the solution, $\boldsymbol{u}$ is obtained from

$$\begin{pmatrix} \frac{\partial^2 F}{\partial u^2} & \frac{\partial^2 F}{\partial u \partial v} & \frac{\partial^2 F}{\partial u \partial w} \\ \frac{\partial^2 F}{\partial u \partial v} & \frac{\partial^2 F}{\partial v^2} & \frac{\partial^2 F}{\partial u \partial w} \\ \frac{\partial^2 F}{\partial u \partial w} & \frac{\partial^2 F}{\partial v \partial w} & \frac{\partial^2 F}{\partial w^2} \end{pmatrix} \begin{bmatrix} \Delta u \\ \Delta v \\ \Delta w \end{bmatrix} = \begin{bmatrix} -\frac{\partial F}{\partial u} \\ -\frac{\partial F}{\partial v} \\ -\frac{\partial F}{\partial w} \end{bmatrix}$$

The solution at the nth iteration step is updated using

$$\boldsymbol{u}^{n+1} = \boldsymbol{u}^n + (\Delta \boldsymbol{u})^n, \tag{13}$$

where the superscripts denote the iteration level. The procedure is repeated until convergence is achieved within a specified tolerance. For the four-sensor probe an initial guess was obtained by treating the probe as two x-arrays. For a brief description of the calibration of an x-probe the reader is referred to Wygnanski et al. (1986).

For the results presented in this article, the solution was usually obtained within five iterations. A solution that took ten or more iterations to converge was rarely a physical one; therefore, the iterations were stopped at ten and that point would be flagged to be rejected. For every point the pitch and yaw angles were calculated to make sure they were within the calibration range.

The calibration data were tested to see whether the calibration velocities were recovered from the bridge voltages. The velocities were usually recovered to within less than 0.5% and never within more than 1%.

4.2 Nonuniform velocity in the sensing volume – the twelve-sensor probe

When a multi-sensor probe is used in a non-uniform flow, the velocity vector seen by each sensor will be different. In a turbulent flow, the flow detected by a multiple-sensor probe is not uniform across the sensing volume. The effects of the velocity gradients on multiple-sensor probe performances have been demonstrated by Vukoslavčević and Wallace (1981) and Park and Wallace (1992).Vukoslavčević et al. (1991) used a nine-sensor probe to measure the spanwise and cross-stream velocity gradients in addition to the three components of the instantaneous velocity vector in a turbulent boundary-layer. They calculated the streamwise gradients from the temporal gradients using Taylor's hypothesis (Piomelli et al. 1989), and thus were able to obtain all three components of the instantaneous vorticity vector as well. The twelve-sensor probe is an extension of the nine-sensor probe and the extra sensors were added to widen the cone of acceptance and to eliminate some of the uniqueness problems. Dracos et al. (1989) presented results obtained with a twelve-sensor probe, but their calibration and reduction algorithm was quite different from the present one. The data reduction for the twelve-sensor probe follows a very similar procedure to that of the four-sensor probe presented earlier, except now the gradients across the sensing volume are taken into account. Following Vukoslavčević et al. (1991) we expand the velocity measured by each wire, $\boldsymbol{u}_j$, in a Taylor series to first order around the centroid of the frontal area of the probe. Hence we let

$$\boldsymbol{u}_j = \boldsymbol{u} + c_j \frac{\partial \boldsymbol{u}}{\partial y} + d_j \frac{\partial \boldsymbol{u}}{\partial z}, \tag{14}$$

where the right-hand-side is evaluated at the probe centroid. The constants c_j and d_j are the vertical and horizontal distances from the centroid of each wire to the centroid of the probe respectively. Thus, in this procedure, instead of the velocity, the velocity *gradient* is assumed to be uniform across the sensing volume. Substitution of Eq. (14) into Eq. (11) yields twelve nonlinear algebraic

equations given by

$$f_j \equiv -P_j + u^2 + 2c_j u\frac{\partial u}{\partial y} + 2d_j u\frac{\partial u}{\partial z}$$
$$-K_{1j}\left[v^2 + 2c_j v\frac{\partial v}{\partial y} + 2d_j v\frac{\partial v}{\partial z}\right]$$
$$-K_{2j}\left[w^2 + 2c_j w\frac{\partial w}{\partial y} + 2d_j w\frac{\partial w}{\partial z}\right]$$
$$-K_{3j}\left[uv + c_j\left(u\frac{\partial v}{\partial y} + v\frac{\partial u}{\partial y}\right) + d_j\left(u\frac{\partial v}{\partial z} + v\frac{\partial u}{\partial z}\right)\right]$$
$$-K_{4j}\left[uw + c_j\left(u\frac{\partial w}{\partial y} + w\frac{\partial u}{\partial y}\right) + d_j\left(u\frac{\partial w}{\partial z} + w\frac{\partial u}{\partial z}\right)\right]$$
$$-K_{5j}\left[vw + c_j\left(v\frac{\partial w}{\partial y} + w\frac{\partial v}{\partial y}\right) + d_j\left(v\frac{\partial w}{\partial z} + w\frac{\partial v}{\partial z}\right)\right] = 0,$$

with the 9 unknowns

$$U \equiv U_k \equiv \left(u, v, w, \frac{\partial u}{\partial y}, \frac{\partial u}{\partial z}, \frac{\partial v}{\partial y}, \frac{\partial v}{\partial z}, \frac{\partial w}{\partial y}, \frac{\partial w}{\partial z}\right). \tag{16}$$

The nonlinear system can be solved in a least-squares sense using Newton's method, where the error defined by Eq. (12) is minimized. The incremental correction to the solution at the nth iteration step can be computed from the 9×9 linear system.

$$\mathbf{H} \cdot \Delta U = -G, \tag{17}$$

where

$$G \equiv \frac{\partial F}{\partial U_k} \tag{18}$$

is the gradient vector consisting of the derivative of F with respect to each of the unknowns, and

$$\mathbf{H} \equiv \frac{\partial^2 F}{\partial U_i \partial U_k} \tag{19}$$

is the Hessian matrix composed of all possible second derivatives of F with respect to the unknowns. An initial guess for the velocity components was obtained by treating each four-wire array as two x-probes. The initial gradients were computed by differencing the velocities from the three four-wire arrays. Convergence, within a specified tolerance, was achieved within five iterations. The pitch and yaw angles encountered by each sensor were checked *a posteriori* in order to verify the integrity of the solution. The points that were outside the calibration range were rejected.

The data reduction procedure was also applied to the calibration data. The velocities were usually recovered to within less than 0.5% and never within more than 1%. Since the probe was calibrated in uniform flow, the calibration data should ideally yield no velocity gradients. The spurious velocity gradient components obtained from the calibration data were usually less than $10\ s^{-1}$ and never more than $20\ s^{-1}$.

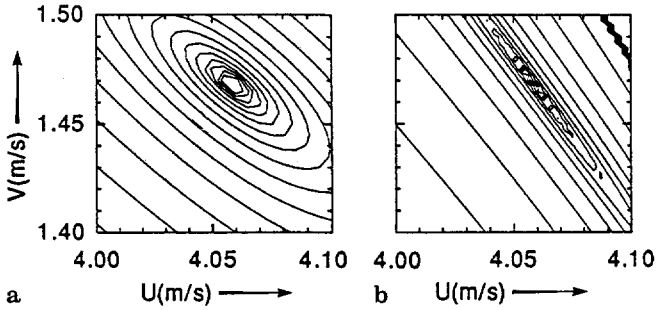

Fig. 6a and b. Contours of the error defined by Eq. (12) using **a** four sensors; **b** three sensors

Note that the present calibration and data reduction scheme can easily be applied to probes with different geometries. The only geometrical information needed is the distance from the center of each wire to the centroid of the frontal sensing area of the probe. The number of sensors need not be fixed at twelve.

4.3 Uniqueness of the solutions

Here, we shall briefly demonstrate the uniqueness of the four-sensor solutions by examining the convergence process in some detail. For this purpose we shall consider the velocity vector with the highest pitch and yaw angles used in the calibration at $+20°$ pitch and $-20°$ yaw. Figure 6(a) shows the contours of the error as defined by Eq. (12). The error contours are plotted in the u-v plane; the w component of the velocity was eliminated using one of the equations represented by Eq. (11). The unique minimum in the error corresponds to the physical solution and is converged to within a few iterations. Similar contours are depicted in Fig. 6(b) for the same velocity data by disregarding one of the wires in the four-sensor probe thus yielding a triple-sensor configuration. The resulting error contours show a valley of possible solutions without a clear minimum. In this case the algorithm iterated numerous times jumping from one solution *well* to another. For the turbulence data acquired by the four-sensor probe the error contours were of the type presented in Fig. 6(a). For the twelve-sensor probe, each four-sensor array was treated as a four-sensor probe and the uniqueness of the solution was determined to the leading order (ignoring the gradients).

5 Velocity and vorticity measurements in the wake of a circular cylinder

The performance of the four- and twelve-sensor probes was tested in the wake of a 6.35 mm diameter circular

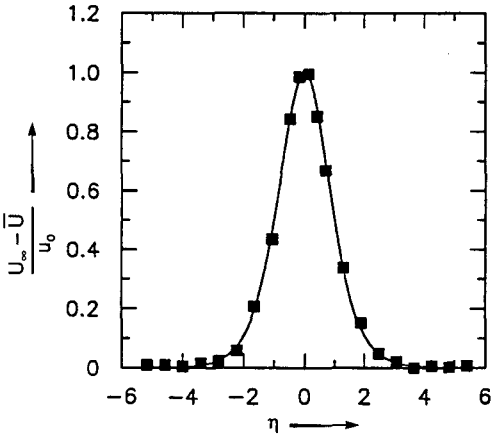

Fig. 7. The normalized mean velocity profile in the circular cylinder wake at $x/d = 30$. Measurements with: ——, the four-sensor probe; ■, the twelve-sensor probe

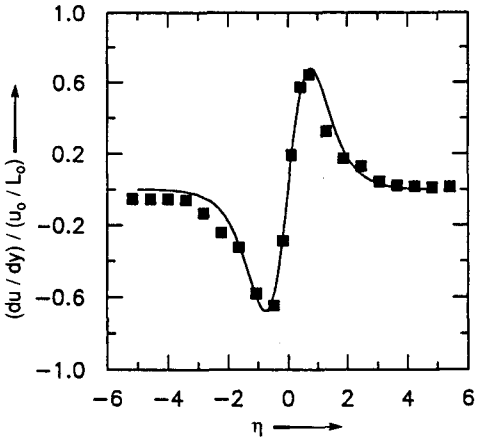

Fig. 8. The mean velocity gradient directly measured by the twelve-sensor probe (■) in the circular cylinder wake and comparison with the derivative of the mean velocity profile (——)

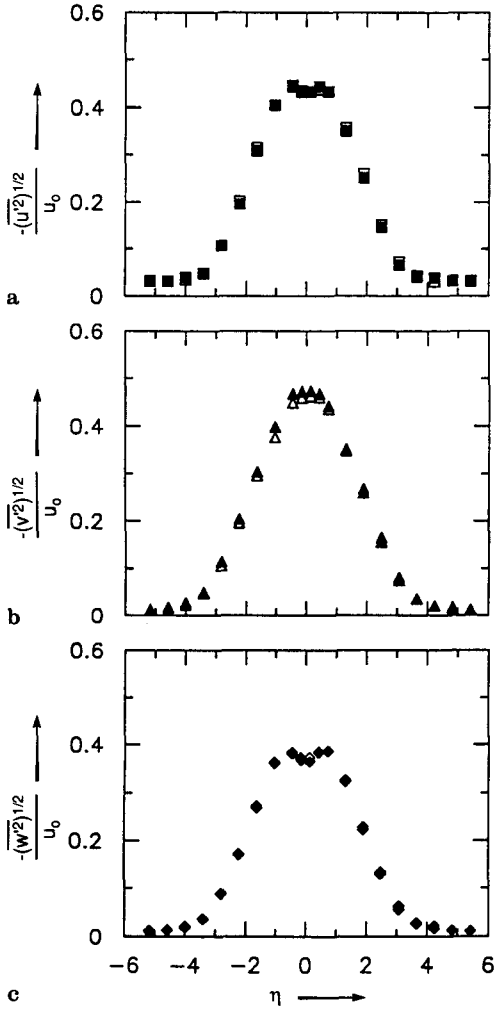

Fig. 9a–c. Turbulence intensity profiles in the circular cylinder wake at $x/d = 30$. The light symbols represent the measurements with the four-sensor probe and the dark symbols correspond to the measurements with the twelve-sensor probe

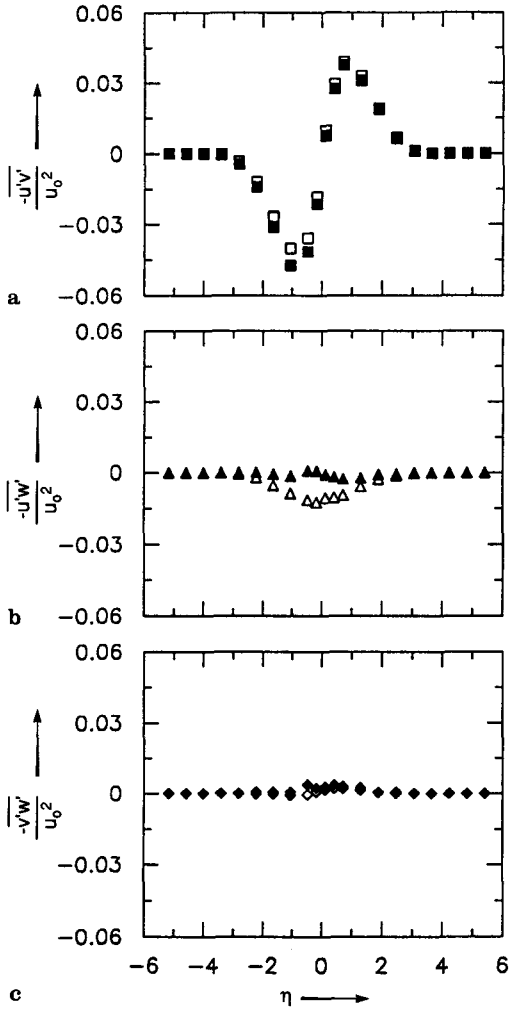

Fig. 10a–c. Reynolds shear stress profiles in the circular cylinder wake at $x/d = 30$. The light symbols represent the measurements with the four-sensor probe and the dark symbols correspond to the measurements with the twelve-sensor probe

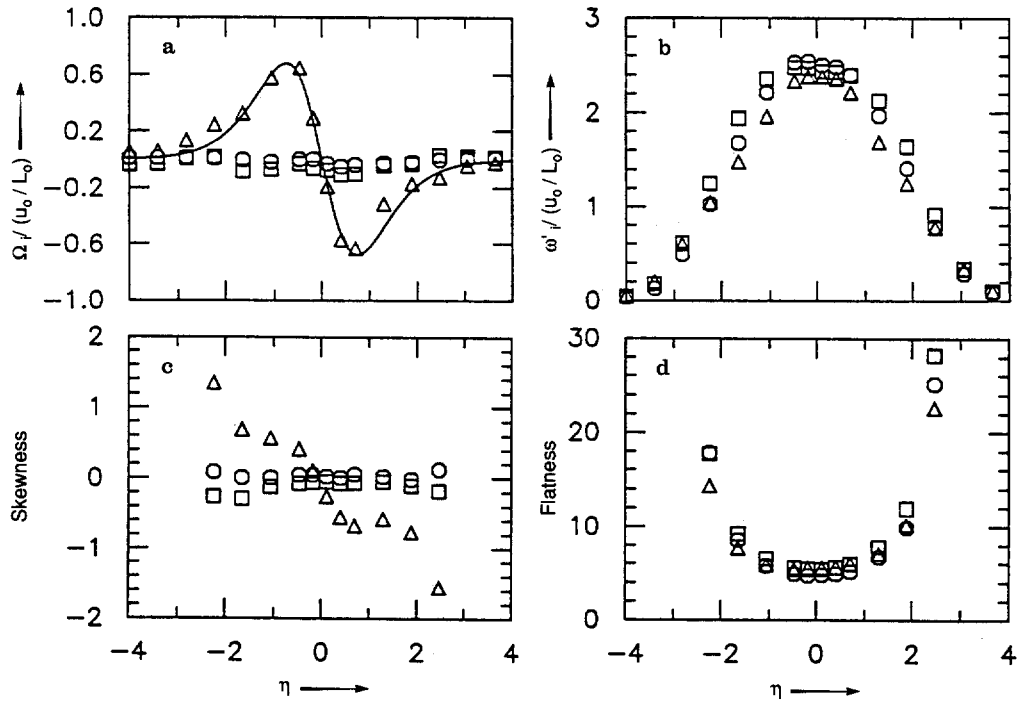

Fig. 11a–d. Distribution of **a** the mean vorticity; **b** the rms vorticity components ω_i'; **c** the skewness factor; and **d** the flatness factor across the wake. □, streamwise; ⊙, cross-stream; △, spanwise components; ———, $-d\bar{U}/dy$.

cylinder. The probe was placed downstream of the cylinder at the location $x/d = 30$. The free stream velocity was $U_\infty = 5$ m/s, resulting in a Reynolds number of 2000 based on the diameter.

The mean velocity profile is shown in Fig. 7. The abscissa, $\eta \equiv y/L_0$, is the vertical coordinate normalized by the half-width of the wake, L_0, which was 8.5 mm. The ordinate is the velocity deficit normalized by the centerline value $u_0 = 0.82$ m/s. The momentum thickness, θ, which is proportional to the drag of the cylinder, was 2.8 mm. In Fig. 7 the symbols represent the measurements with the twelve-sensor probe and the solid curve corresponds to a curve fit to the measurements with the four-sensor probe. The profile is quite symmetric around the centerline, as it should be.

Figure 8 compares the distribution of the mean velocity gradient $\partial\bar{U}/\partial y$ measured directly with the twelve-sensor probe with the derivative of the curve fit to the $\bar{U}$ distribution shown in Fig. 7. The excellent agreement between the two shows the capability of this probe to measure instantaneous velocity gradients accurately, which is essential for vorticity measurements.

The turbulence intensities of the u (streamwise or x-direction), v (cross-stream or y-direction) and w (spanwise or z-direction) velocity components are shown in Fig. 9. Here the dark symbols represent the twelve-sensor data while the light symbols correspond to the four-sensor data. At the centerline the v component has the most intense fluctuations, which is due to the von Karman vortex shedding present in the flow. The Reynolds shear stresses are presented in Fig. 10. Ideally $-\overline{u'w'}$ and $-\overline{v'w'}$ should be identically zero because of the symmetry of the flow geometry. The twelve-sensor probe gives much smaller $-\overline{u'w'}$ than the four-sensor probe. The data presented in Figs. 9 and 10 are in agreement with previously reported results (see for example Yamada et al. 1980).

Figure 11 depicts the vorticity statistics measured by the twelve sensor probe. The mean vorticity values of $\bar{\Omega}_x$ and $\bar{\Omega}_y$ shown in Fig. 11(a), are approximately zero as required for this two-dimensional wake flow. The directly measured $\bar{\Omega}_z$ is very close to that obtained by differentiating the measured mean streamwise velocity profile. The maximum rms values of the vorticity components have quite high signal-to-noise ratios, and they peak at the wake centerline as seen in Fig. 11(b). All three components have similar distributions across the wake. The skewness and flatness factors are displayed in Figs. 11(c, d). The range is limited to within $\pm 2.5\ L_0$, because the intermittent region of the wake produces extremely high values. The skewness factors for ω_x and ω_y are nearly zero across the wake, consistent with the two-dimensional nature of the mean flow. The ω_z skewness factor is positive for the lower wake, crosses zero at the centerline, and is negative for the upper wake, consistent with the sign of $\bar{\Omega}_z$.

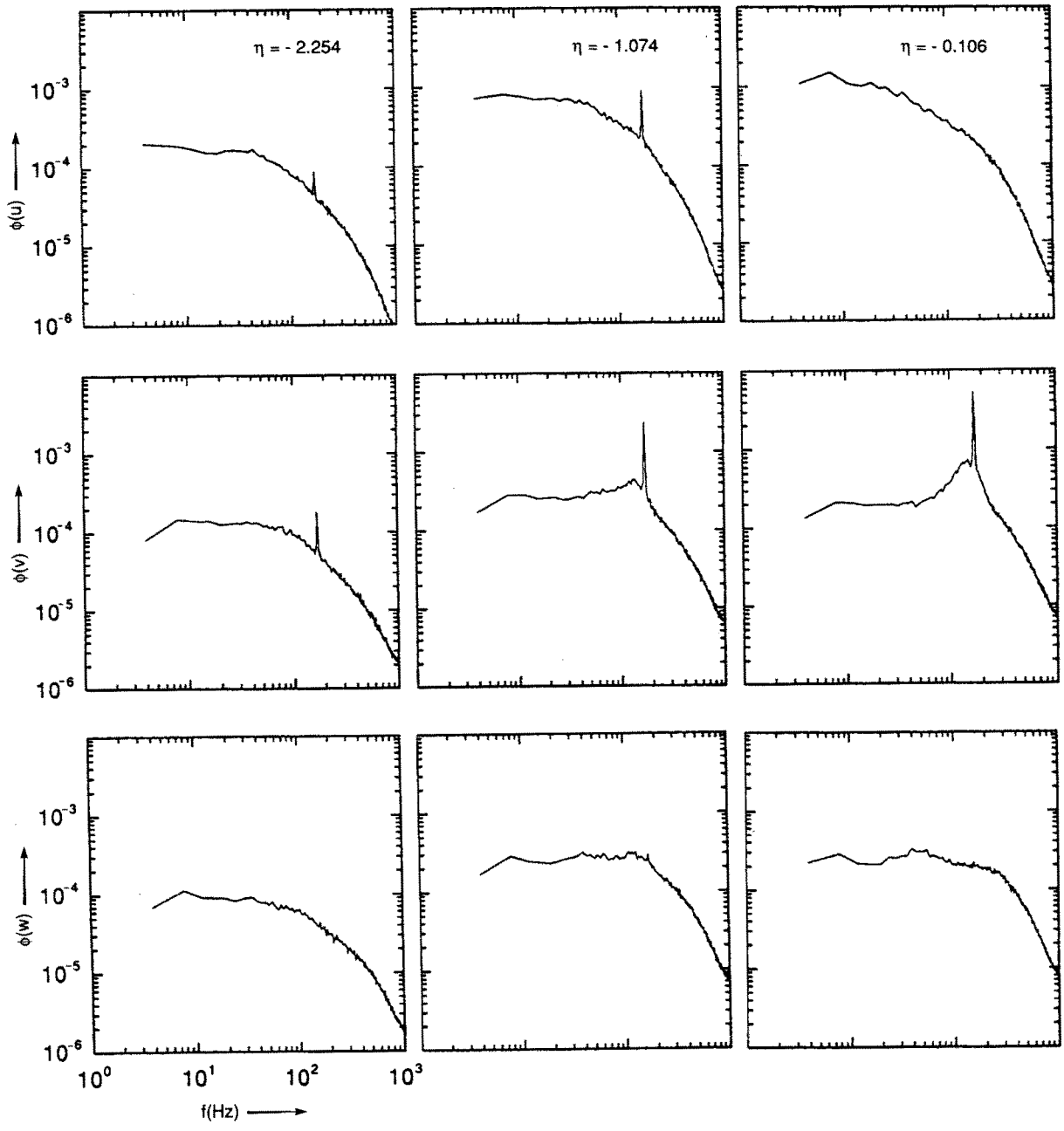

Fig. 12. Velocity spectra obtained from the twelve-sensor probe measurements in the circular cylinder wake at various cross-stream locations

The flatness factors are approximately the same for all three components, and are about 5.0 in the centerline region.

The power spectra of the velocity fluctuations measured by the twelve-sensor probe at three different cross-stream locations are shown in Fig. 12. The sharp peaks in the spectra correspond to the von Karman vortex shedding, which occurs at 168 Hz or Strouhal number, $St = f_s d/U_\infty = 0.21$. The shedding is most evident in the v-spectra and nonexistent in the w-spectra, which is an indication of the nominal two-dimensionality of the flow. The vorticity spectra are shown in Fig. 13. Here the peak at f_s is noticeably absent from the ω_x and ω_y spectra, but is evident in the ω_z spectra, demonstrating both the two-dimensionality of the shedding and the ability of the probe to resolve the different components of the vorticity.

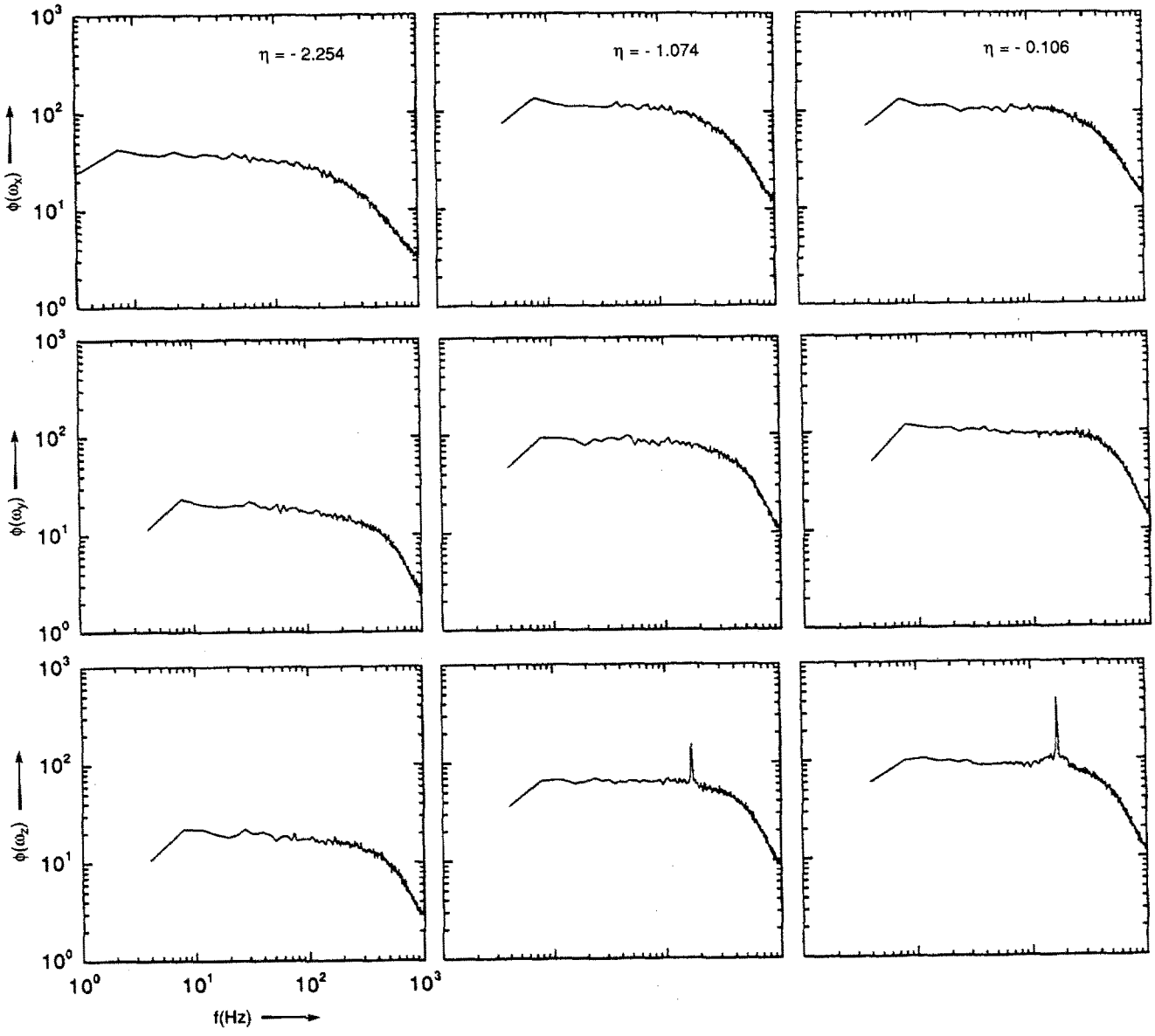

Fig. 13. Vorticity spectra obtained from the twelve-sensor probe measurements in the circular cylinder wake at various cross-stream locations

6 Conclusions

To our knowledge, this is the first documentation of the simultaneous measurement of all three components of the velocity and all three components of the vorticity vectors in a wake flow. A calibration scheme which requires no information about the probe geometry was introduced and was tested using a four-sensor and a twelve-sensor probe. Two data reduction algorithms were introduced. The first one assumed uniform velocity over the probe sensing-volume and was applied to the four-sensor probe measurements. The second one assumed uniform velocity gradient over the sensing volume of the probe. The procedure, when applied to the twelve-sensor probe, was shown to measure the velocity gradients successfully. In both algorithms, the unknowns (velocity and velocity gradient components) were obtained by solving the resulting systems of nonlinear algebraic equations in a least-squares sense. For the range of pitch and yaw angles used ($\pm 20°$) the velocity components were uniquely determined. The detection of the von Karman shedding frequency only in the spanwise vorticity spectra indicated that the vorticity components were satisfactorily resolved.

Appendix

Given the bridge voltage e_i corresponding to the known calibration velocity components u_i, v_i and w_i ($i=1, N_c$), where N_c is number of calibration points, the unknown coefficients in the sensor response equation (Eq. (6)) can be determined from the following linear system of equations:

$$\begin{pmatrix}
N_c & \bar{e} & \overline{e^2} & \overline{e^3} & \overline{e^4} & \overline{v^2} & \overline{w^2} & \overline{uv} & \overline{uw} & \overline{vw} \\
\bar{e} & \overline{e^2} & \overline{e^3} & \overline{e^4} & \overline{e^5} & \overline{ev^2} & \overline{ew^2} & \overline{euv} & \overline{euw} & \overline{evw} \\
\overline{e^2} & \overline{e^3} & \overline{e^4} & \overline{e^5} & \overline{e^6} & \overline{e^2v^2} & \overline{e^2w^2} & \overline{e^2uv} & \overline{e^2uw} & \overline{e^2vw} \\
\overline{e^3} & \overline{e^4} & \overline{e^5} & \overline{e^6} & \overline{e^7} & \overline{e^3v^2} & \overline{e^3w^2} & \overline{e^3uv} & \overline{e^3uw} & \overline{e^3vw} \\
\overline{e^4} & \overline{e^5} & \overline{e^6} & \overline{e^7} & \overline{e^8} & \overline{e^4v^2} & \overline{e^4w^2} & \overline{e^4uv} & \overline{e^4uw} & \overline{e^4vw} \\
\overline{v^2} & \overline{ev^2} & \overline{e^2v^2} & \overline{e^3v^2} & \overline{e^4v^2} & \overline{v^4} & \overline{v^2w^2} & \overline{uv^3} & \overline{uv^2w} & \overline{v^3w} \\
\overline{w^2} & \overline{ew^2} & \overline{e^2w^2} & \overline{e^3w^2} & \overline{e^4w^2} & \overline{v^2w^2} & \overline{w^4} & \overline{uvw^2} & \overline{uw^3} & \overline{vw^3} \\
\overline{uv} & \overline{euv} & \overline{e^2uv} & \overline{e^3uv} & \overline{e^4uv} & \overline{uv^3} & \overline{uvw^2} & \overline{u^2v^2} & \overline{u^2vw} & \overline{uv^2w} \\
\overline{uw} & \overline{euw} & \overline{e^2uw} & \overline{e^3uw} & \overline{e^4uw} & \overline{uv^2w} & \overline{uw^3} & \overline{u^2vw} & \overline{u^2w^2} & \overline{uvw^2} \\
\overline{vw} & \overline{evw} & \overline{e^2vw} & \overline{e^3vw} & \overline{e^4vw} & \overline{v^3w} & \overline{vw^3} & \overline{uv^2w} & \overline{uvw^2} & \overline{v^2w^2}
\end{pmatrix}
\begin{bmatrix} A_0 \\ A_1 \\ A_2 \\ A_3 \\ A_4 \\ K_1 \\ K_2 \\ K_3 \\ K_4 \\ K_5 \end{bmatrix}
=
\begin{bmatrix} \overline{u^2} \\ \overline{eu^2} \\ \overline{e^2u^2} \\ \overline{e^3u^2} \\ \overline{e^4u^2} \\ \overline{u^2v^2} \\ \overline{u^2w^2} \\ \overline{u^3v} \\ \overline{u^3w} \\ \overline{u^2vw} \end{bmatrix}$$

where

$$\bar{e}=\sum_{i=1}^{N_c} e_i, \qquad \overline{e^2}=\sum_{i=1}^{N_c} e_i^2,$$

etc.

Acknowledgements

We would like to thank Dr. P. Vukoslavčević who constructed the probes and Dr. L. Ong who assisted in the data acquisition process. P. N. would like to acknowledge the sponsorship of Drs. F. Peterson and B. Douglas at DTMB. Funding was provided to B. M. by the Air Force Engineering Foundation Grant RI-B-90-14 and to J. W. by NSF Grant CTS-891189 and DOE Grant DEFG05-88ER13838.

References

Adrian, R. J.; Johnson, R. E.; Jones, B. G.; Merati, P.; Tung, T. C. 1984: Aerodynamic disturbances of hot wire probes and directional sensitivity. J. Phys. E: Sci. Instrum. 17, 62–71

Döbbeling, K.; Lenze, B.; Leuckel, W. 1990: Basic considerations concerning the construction and usage of multiple hot-wire probes for highly turbulent three-dimensional flows. Meas. Sci. Technol. 1, 924–933

Dracos, T.; Kholmyansky, M.; Kit, E.; Tsinober, A. 1989: Some experimental results on velocity-velocity gradients measurements in turbulent grid flows. In: Topological Fluid Mechanics. (eds. Moffatt, H. K.; Tsinober, A.), pp. 564–584. Cambridge: Cambridge University Press.

Jorgensen, F. E. 1971: Directional sensitivity of wire and fiber film probes. DISA Inform. 11, 31–37

King, L. V. 1914: On the convection of heat from small cylinders in a stream of fluid. Phys. Trans. R. Soc. Lond. A214, 373–432.

Lekakis, I. C.; Adrian, R. J.; Jones, B. G. 1989: Measurement of velocity vectors with orthogonal and non-orthogonal triple-sensor probes. Exp. Fluids 7, 228–240

Park, S.-R.; Wallace, J. M. 1992: The influence of velocity gradients on turbulence properties measured with multi-sensor hot-wire probes. Proceedings of the Thirteenth Symposium on Turbulence, University of Missouri-Rolla, USA

Piomelli, U.; Balint, J.-L.; Wallace, J. M. 1989: On the validity of Taylor's hypothesis for wall-bounded turbulent flows. Phys. Fluids A 1, 609–611

Samet, M.; Einav, S. 1987: A hot-wire technique for simultaneous measurement of instantaneous velocities in 3D flows. J. Phys. E: Sci. Instrum. 20, 683–690

Vagt, J.-D. 1979: Hot-wire probes in low speed flow. Prog. Aerospace Sci. 18, 271–323

Vukoslavčević, P.; Wallace, J. M. 1981: Influence of velocity gradients on measurements of velocity and streamwise vorticity with hot-wire x-array probes. Rev. Sci. Instrum. 52(6), 869–879

Vukoslavčević, P.; Wallace, J. M.; Balint, J.-L. 1991: The velocity and vorticity vector fields of a turbulent boundary layer. Part 1. Simultaneous measurement by hot-wire anemometry. J. Fluid Mech. 228, 25–51

Wygnanski, I.; Champagne, F.; Marasli, B. 1986: On the large-scale structures in a two-dimensional, small-deficit, turbulent wakes. J. Fluid Mech. 168, 31–71

Yamada, H.; Kawata, Y.; Osaka, H.; Kageyama, Y. 1980: Turbulence Measurements in a two-dimensional turbulent wake. Tech. Rep. Yamaguchi University, Japan 2, 329–339